Monthly Notices
of the
ROYAL ASTRONOMICAL SOCIETY

MNRAS **480,** 3864–3870 (2018)
Advance Access publication 2018 August 8

doi:10.1093/mnras/sty2155

A transiting M-dwarf showing beaming effect in the field of Ruprecht 147

Philipp Eigmüller,[1,2] Szilárd Csizmadia,[1] Michael Endl,[3] Davide Gandolfi,[4] William D. Cochran,[3] David Yong,[5] Alexis M. S. Smith,[1] Juan Cabrera,[1] Hans J. Deeg,[6,7] Marshall C. Johnson,[8] Judith Korth,[9] David Nespral,[6,7] Jorge Prieto-Arranz[6,7] and Artie P. Hatzes[10]

[1]*Institute of Planetary Research, German Aerospace Center, Rutherfordstrasse 2, D-12489 Berlin, Germany*
[2]*Center for Astronomy and Astrophysics, TU Berlin, Hardenbergstr. 36, D-10623 Berlin, Germany*
[3]*Department of Astronomy and McDonald Observatory, University of Texas at Austin, 2515 Speedway, Stop C1400, Austin, TX 78712, USA*
[4]*Dipartimento di Fisica, Universitá di Torino, via P. Giuria 1, I-10125 Torino, Italy*
[5]*Research School of Astronomy and Astrophysics, The Australian National University, Cotter Road, Canberra, ACT 2611, Australia*
[6]*Instituto de Astrofísica de Canarias, C. Vía Láctea S/N, E-38205 La Laguna, Tenerife, Spain*
[7]*Departamento de Astrofísica, Universidad de La Laguna, E-38206 La Laguna, Tenerife, Spain*
[8]*Department of Astronomy, The Ohio State University, 140 West 18th Ave., Columbus, OH 43210, USA*
[9]*Rheinisches Institut für Umweltforschung an der Universität zu Köln, Aachener Strasse 209, D-50931Köln, Germany*
[10]*Thüringer Landessternwarte Tautenburg, D-07778 Tautenburg, Germany*

Accepted 2018 August 6. Received 2018 August 6; in original form 2018 June 28

ABSTRACT

We report the discovery and characterization of an eclipsing M5Vdwarf star, orbiting a slightly evolved F7V main sequence star. In contrast to previous claims in the literature, we confirm that the system does not belong to the galactic open cluster Ruprecht 147. We determine its fundamental parameters combining K2 time-series data with spectroscopic observations from the McDonald Observatory, FIES@NOT, and HIRES@KECK. The very precise photometric data from the K2 mission allows us to measure variations caused by the beaming effect (relativistic doppler boosting), ellipsoidal variation, reflection, and the secondary eclipse. We determined the radial velocity using spectroscopic observations and compare it to the radial velocity determined from the beaming effect observed in the photometric data. The M5V star has a radius of $0.200^{+0.007}_{-0.008}$ $R_\odot$ and a mass of $0.187^{+0.012}_{-0.013}$ $M_\odot$. The primary star has a radius of $1.518^{+0.038}_{-0.049}$ $R_\odot$ and a mass of $1.008^{+0.081}_{-0.097}$ $M_\odot$. The orbital period is 5.441995 ± 0.000007 d. The system is one of the few eclipsing systems with observed beaming effect and spectroscopic radial velocity measurements and it can be used as a test case for the modelling of the beaming effect. Current and forthcoming space missions such as *TESS* and *PLATO* might benefit from the analysis of the beaming effect to estimate the mass of transiting companions without the need for radial velocity follow up observations, provided that the systematic sources of noise affecting this method are well understood.

Key words: binaries: eclipsing – stars: fundamental parameters – stars: low-mass.

1 INTRODUCTION

To understand the evolution of stars and planetary systems it is fundamental to derive observationally the fundamental parameters of stars in different stages of their evolution and compare those results with stellar evolution models. Although low mass stars with a mass well below one solar mass are most common in our solar neighbourhood, they are not yet completely understood, even in regards to their bulk parameters. They show significant discrepancies between theoretical and observed mass–radius relation. For very low mass stars (VLMSs) in a mass regime between 0.1 and 0.6 $M_\odot$ Mann et al. (2015) found that Dartmouth models (Dotter et al. 2008) systematically underestimate the radius by ≈4.7 per cent and overestimate the effective temperature by ≈2.2 per cent.

One key observational method to determine the mass and radius of low mass stars is the study of detached eclipsing binaries (DEBs). The DEBCat catalogue (Southworth 2015) of DEBs lists currently 29[1] well characterized VLMSs with a mass below 0.6 $M_\odot$.

* E-mail: philipp.eigmueller@dlr.de

[1] http://www.astro.keele.ac.uk/jkt/debcat; state of June 2018

DEBcat is limited to DEBs with their bulk parameters determined to a precision better than 2 per cent. Many more DEBs not as well characterized are known (e.g. Eigmüller et al. 2016; Gillen et al. 2017; Chaturvedi et al. 2018).

In this paper we present the detailed characterization of a DEB formed by a main sequence star and an M dwarf companion with precise *K2* photometry and ground-based radial velocity follow-up.

We deduce the bulk characteristics of an M dwarf companion to a solar-like star modelling *K2* light curve and radial velocity follow up measurements. The high-precision light curves by the *Kepler* satellite allow us not only to model the primary eclipse but also to model the occultation as well as reflection, ellipsoidal variation, and the relativistic beaming effect. Due to the high contrast ratio between late- and early-type stars, secondary eclipse of M dwarfs are only rarely observed in such systems. The observation of the secondary eclipse and reflection allows us to give additional constrains on the luminosity ratio in the binary system, and the albedo of the M dwarf. The ellipsoidal variation depends mainly on the mass ratio of the two components and the semimajor axis of the system, and thus also gives further constrains on the system parameters.

1.1 Relativistic beaming

The relativistic beaming effect is caused by the reflex motion of the stars introducing photometric flux variations due to the Doppler effect. The theoretical background of the relativistic beaming effect has been discussed for eclipsing binary stars (Zucker, Mazeh & Alexander 2007) as well as for planetary systems (Loeb & Gaudi 2003). Using light curves of CoRoT (Convection, Rotation, and planetary Transits) and the *Kepler* satellite, a few observations of this effect have been reported in the last years (Mazeh & Faigler 2010; van Kerkwijk et al. 2010; Bloemen et al. 2011; Herrero et al. 2014; Faigler et al. 2015; Tal-Or, Faigler & Mazeh 2015). For a few transiting systems (Mazeh & Faigler 2010; Bloemen et al. 2011; Faigler et al. 2015) and even more non-transiting systems (Tal-Or et al. 2015) spectroscopic radial velocity measurements are available.

The measurement of the relativistic beaming effect allows an independent estimate of the radial velocity of the secondary component of the binary system, which can be used to establish the nature of the companion and to determine the mass ratio between primary and secondary objects.

This effect has been proposed in the literature as a tool to confirm the nature of transiting planetary companions, which otherwise typically require an extensive ground-based follow-up campaign to confirm their nature. The scheduling of ground-based resources is one of the current challenges for space-borne transit surveys like *K2* or, in the future missions, Transiting Exoplanet Survey Satellite (TESS) and PLATO (Planetary Transits and Oscillations of stars). Understanding the limitations of relativistic beaming effect will allow to establish this method as an independent tool to identify low mass stellar companions, one of the main sources of false-positives for transit surveys. Unfortunately, as it will be shown in this paper, the current state-of-the-art approach neglects the influence of stellar variability, which might compromise the retrieval of the radial velocity value from the photometry (Faigler et al. 2015; Csizmadia submitted). In case of disagreement between the radial velocity amplitudes between photometry and spectroscopy, the latter value is preferred.

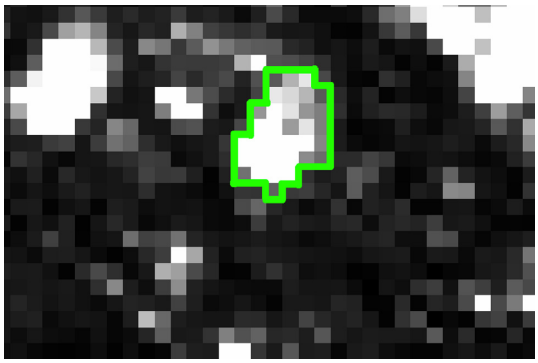

Figure 1. Stamp of K2 observation of this object. The green line shows the aperture selected for photometry.

2 OBSERVATIONS

2.1 K2 photometry and transit detection

The *Kepler* space observatory, launched in 2009, was designed to provide precise photometric monitoring of over 150 000 stars in a single field and to detect transiting Earth-sized planets with orbital periods up to 1 yr (Borucki et al. 2010). Due to failure of two reaction wheels the Kepler mission stopped after 4 yr of operation. At the end of 2013 the operation of the *Kepler* space telescope re-started with a new concept that uses the remaining reaction wheels, the spacecraft thrusters, and solar wind pressure, to point the telescope. The new mission, called K2 (Howell et al. 2014), enables the continued use of the *Kepler* spacecraft with limited pointing accuracy. K2 observes different fields located along the ecliptic for a duration of about three consecutive months per field. Ruprecht 147 is an open cluster observed with K2 during Campaign 7. It was observed using a super-aperture, tiled with 60 51x51 masks, totalling 156 060 pixels.

For the photometry we combined the single masks to the super-aperture for all 4043 frames. A master frame, combined out of all 4043 frames, was used to identify sources and their individual masks using the label function in the python scipy module. The photometry was performed using a fixed aperture for each object as described in Eigmüller et al. (2017). Similar to the Kepler pipeline of Vanderburg & Johnson (2014), each light curve was split in segments to remove noise correlated with the pointing of the *Kepler* spacecraft. For the transit detection we used the DST algorithm described in Cabrera et al. (2012). This algorithm has been largely used by our team to detect planets in other K2 fields (Barragán et al. 2016; Grziwa et al. 2016a; Johnson et al. 2016; Eigmüller et al. 2017; Smith et al. 2017). EPIC 219654213 was identified as possible planetary candidate and radial velocity follow up observations were scheduled to determine the mass of the companion. These observations allowed us to characterize the companion as M5V star.

For the modelling of the light curve we re-analysed the photometry with optimal selected aperture size and customized segment size for de-correlation. We tested different aperture sizes and finally selected by manual inspection the aperture as shown in Fig. 1. The size of the segments for decorrelation and detrending has been selected to be twice the orbital period of the EB. This way we avoid splitting the light curve within any eclipse signal. These short segments were individually de-correlated against the relative motion of the star, given in the `POS_CORR` columns. To remove long-term trends we de-correlated these segments also in the time domain for linear trends. The resulting light curve, in the time domain and phase folded, is shown in Fig. 2. In a last step we removed outliers

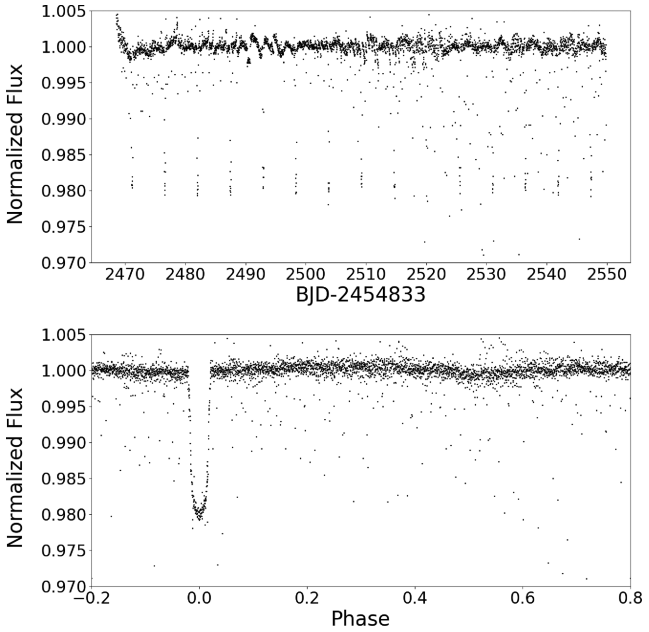

Figure 2. Corrected and normalized light curve of EPIC 219654213. The upper plot shows the raw normalized light curve over time, with long-term trends removed. The lower plot displays the same data, phase folded to the orbital period.

and the ramp at the beginning of the light curve.

2.2 High dispersion spectroscopy

Spectroscopic radial velocity follow up has been carried out to verify the nature of the companion. We used the Tull Spectrograph at the McDonald Observatory, the FIbre-fed Échelle Spectrograph (FIES) spectrograph at the Nordic Optical Telescope (NOT), and the HIRES Spectrograph (High Resolution Echelle Spectrometer) at the Keck Observatory.

2.3 Tull spectrograph @ McDonald observatory

We observed EPIC 219654213 with the Tull Coudé spectrograph (Tull et al. 1995) at the Harlan J. Smith 2.7 m telescope at McDonald Observatory. The Tull spectrograph images the entire optical spectrum on its Charged-Coupled Device (CCD) detector at a resolving power of $R = 60\,000$. Between 2016 July and 2017 September we collected a total of eight spectra of the star. Exposure times ranged from 20 min to 1 h, depending on seeing conditions. The data were flat-fielded, bias-subtracted, and wavelength-calibrated using standard Image Reduction and Analysis Facility (IRAF) procedures. The extracted spectra have an S/N ratio at 5650 Å between 19 and 36 per 2-pixel resolution element.

For each observation we computed an absolute radial velocity of the star by cross-correlating it with the RV standard star HD 182572 with an absolute RV of $-100.35\,\mathrm{km\,s^{-1}}$ (Jofré et al. 2015). The RV data are listed in Table 1 and displayed in Fig. 6.

2.4 FIES @ NOT

We observed EPIC 219654213 with the FIES (Telting et al. 2014) mounted at the 2.56m NOT of Roque de los Muchachos Observatory (La Palma, Spain). As part of the observing programs 54-205, 54-027, and 55-019, we secured seven intermediate-resolution

Table 1. Tull, FIES, and HARPS-N RV measurements of EPIC 219654213.

BJD_{TDB} $-2\,450\,000$	RV ($\mathrm{km\,s^{-1}}$)	σ_{RV} ($\mathrm{km\,s^{-1}}$)	Instr.
7541.06966767	− 13.13	0.16	HIRES Blue
7542.03177372	1.67	0.65	HIRES Blue
7542.85072551	− 2.87	0.68	Tull
7614.8006962	− 28.5	0.6	HIRES Red
7666.39011879	20.604	0.040	FIES
7668.37494413	21.605	0.027	FIES
7669.37951759	− 0.053	0.071	FIES
7672.60931308	1.79	1.19	Tull
7673.60167106	− 4.45	1.09	Tull
7893.67142075	− 4.773	0.094	FIES
7894.69572934	14.638	0.074	FIES
7895.64675401	31.723	0.043	FIES
7896.70668445	26.071	0.067	FIES
7954.80808902	− 9.93	0.46	Tull
7994.70153193	− 4.84	0.89	Tull
8008.62752647	− 23.38	0.76	Tull
8009.62419535	− 3.09	0.78	Tull
8010.70251742	− 0.24	1.77	Tull

($R \approx 47\,000$) spectra between 2016 October 4 and 2017 May 22 UTC. The exposure time was set to 1200–3600 s, based on our scheduling constrains and sky conditions. We followed the same observing strategy described in Gandolfi et al. (2015) and traced the RV drift of the instrument by bracketing the science exposures with long-exposed (T_{exp}= 35–60 s) ThAr spectra. We reduced the data using standard IRAF and IDL routines and extracted the relative RVs via multi-order cross-correlations with the co-added spectrum of the star .

The extracted spectra have an S/N ratio between 10 and 20 $\mathrm{pixel^{-1}}$ at 5500 Å.

2.5 HIRES @ Keck observatory

HIRES (Vogt et al. 1994) observations were obtained on 2016 June 1 and 2 UTC using the blue configuration. We used the B5 slit (width = 0.86″, length = 3.5″) which provided a resolving power of $R = 49\,000$, and the CCD binning was 2×2. The echelle and cross-disperser angles were set to 0.0 and 0.97, respectively; this provided wavelength coverage from 3030 to 5900 Å. The observing sequence was EPIC 219654213(600s), ThAr lamp, then the radial velocity standard HD 182572 (2×5 s). Data reduction was performed using MAKEE.[2]

An additional HIRES observation was obtained on 2016 August 14 UTC using the red configuration. The B2 slit (width = 0.57″, length = 7.0″) was used providing a resolution of $R = 66\,000$, and the CCD binning was 1×1. The echelle and cross-disperser angles were set to 0.0 and 0.45, respectively, resulting in a wavelength coverage from 4200 to 8500 Å. The observing sequence was EPIC 219654213(600s), the radial velocity standard HD 182572 (2×5 s), then a ThAr lamp. Data reduction was performed using MAKEE. For all exposures, the S/N was 40–50 $\mathrm{pixel^{-1}}$ near 5500 Å for EPIC 219654213. For both sets of observations, the RV was measured by multi-order cross-correlation against HD 182572 (assum-

[2]MAKEE was developed by T. A. Barlow specifically for reduction of Keck HIRES data. It is freely available at http://www2.keck.hawaii.edu/realpublic/inst/hires/data_reduction.html

Table 2. Main identifiers, coordinates, magnitudes, and spectroscopic parameters of the primary star of EPIC 219654213.

Parameter	EPIC 219654213	Unit
RA	$19^h17^m00^s.670$	h
DEC	$-16°11'32''.53$	deg
UCAC4 ID	370-168815	...
EPIC ID	219654213	...
pm RA (GAIA DR2)	1.209 ± 0.048	mas yr^{-1}
pm DEC (GAIA DR2)	-8.619 ± 0.042	mas yr^{-1}
parallax (GAIA DR2)	0.7930 ± 0.0331	mas
Effective temperature $T_{\rm eff}$	6305 ± 110	K
Stellar radius R_1	1.58 ± 0.18	Rsun
Metallicity [Fe/H]	-0.08 ± 0.09	dex
$v \sin i_1$[3]	15.08 ± 0.62	km s^{-1}
Age	4.1 ± 1.1	Gyr
Spectral type	G2 V	–
B mag (UCAC4)	14.533 ± 0.05	mag
V mag (UCAC4)	13.911 ± 0.08	mag
J mag (2MASS)	12.697 ± 0.03	mag
H mag (2MASS)	12.467 ± 0.02	mag
K mag (2MASS)	12.426 ± 0.02	mag

ing -100.35 km s^{-1}; Udry et al. 1999) using the FXCOR package in IRAF (Tody 1993).

3 ANALYSIS

3.1 Spectral analysis

The primary star has been characterized using the SpecMatch-emp tool by Yee, Petigura & von Braun (2017) on a combined FIES spectrum. We empirically determined the effective temperature, metallicity, and radius of the host star. The result is in agreement with an independent spectral analysis using the KEA tool (Endl & Cochran 2016) of a single spectrum taken with the Tull spectrograph. The main parameters of the primary star are listed in Table 2. The effective temperature is 6305 ± 110 K, and the radius is $1.58 \pm 0.18\,R_\odot$.

3.2 Joint analysis of photometric and radial velocity measurements

We used the Transit Light-Curve Modelling (TLCM) code[4] (Csizmadia et al. 2015; Csizmadia submitted) for the analysis of the light curves and radial velocity measurements. TLCM is based on the Mandel & Agol (2002) model to fit planetary transit light curves. The RV measurements are modelled with a Keplerian orbit. The fit is optimized using first a genetic algorithm and then a simulated annealing chain. Uncertainties were estimated from Markov Chain Monte Carlo (MCMC) chains. TLCM is capable of modelling the out-of-transit variations caused by ellipsoidal variation, reflection, and relativistic beaming. To model the beaming the index factors α were calculated by convolving ATLAS spectra at the temperature of the star with the sensitivity curve of K2. Then the flux variations are given as $(1 + \frac{2}{3}\alpha \cdot V_{\rm rad}/c)$ for every phase. The factor of $\frac{2}{3}$ comes from the spherical geometry.

The fitted parameters are the scaled semimajor axis a/R_* and radius ratio $R_{\rm p}/R_*$, the conjunction parameter i, the eccentricity given by $e \cdot sin(\omega)$ and $e \cdot cos(\omega)$, the limb darkening coefficients $u_+ = u_1 + u_2$ and $u_- = u_1 - u_2$, the brightness ratio, the radial velocity semi-amplitude K (from spectroscopic radial velocity data, and the photometric beaming effect combined, but clearly dominated by the spectroscopic data) and the systemic γ-velocity, the ellipsoidal variability, represented by five terms of Legendre polynoms with amplitudes a_j, and the albedo of both components. The period ($P_{\rm orb}$) and epoch of mid-transit (T_0) are allowed to vary slightly around the values determined already by the detection. The contamination factor was determined using the GAIA DR2 information of background objects within our aperture. We also fitted for radial velocity trends that might unveil the presence of additional orbiting companions in the systems. We obtained radial accelerations that are consistent with zero.

The best-fitting transit model is shown in Fig. 3, along with the photometric data. Figs 4 and 5 show expanded views around the primary and secondary transit, respectively. The RV data are shown in Fig. 6. Results of the combined modelling are listed in Table 3.

To retrieve the mass of the primary star we compared Dartmouth stellar models (Dotter et al. 2008).[5] With the effective temperature, metallicity, and radius from spectral classification using

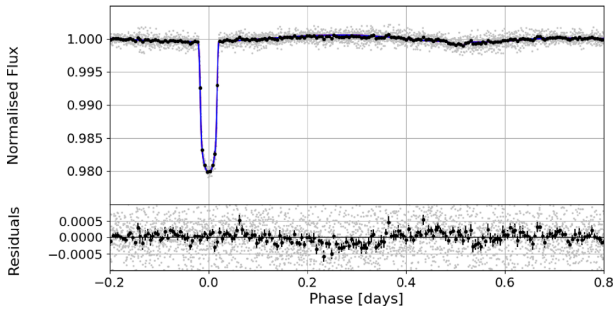

Figure 3. Phase folded light curve and the best-fitting transit model of EPIC 219654213. Grey points are the measurements, black circles the binned data. The continuous line represents the best-fitting model. Residuals to the fit are shown in the lower panel.

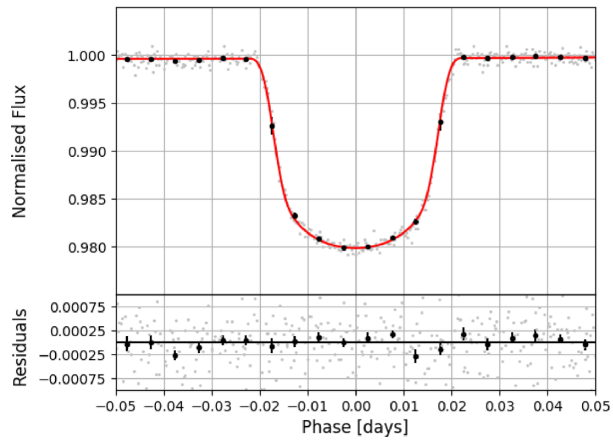

Figure 4. Phase folded light curve of the primary transit and the best-fitting transit model of EPIC 219654213. Grey points are the measurements, black circles the binned data. The continuous red line represents the best-fitting model. Residuals to the fit are shown in the lower panel.

[4]We used the latest version which was tlcm92_f (June, 2018).

[5]Characterization of the primary star using Parsec1.2S isochrones (Bressan etal. 2012) gave results in agreement with our findings using the Dartmouth stellar models.

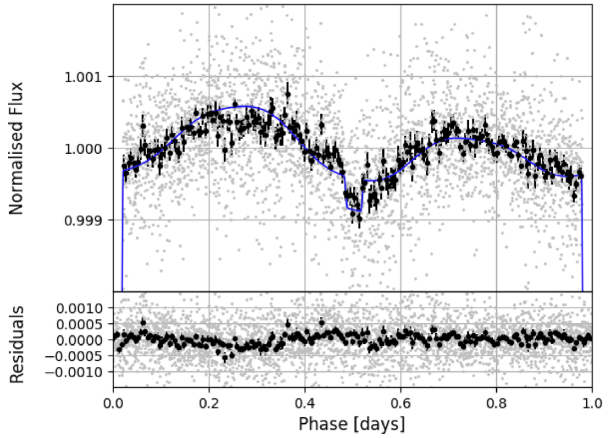

Figure 5. Phase folded light curve with the y-scale adapted to highlight the secondary eclipse and out-of-transit variations. Grey points are the measurements, black circles the binned data. The continuous blue line represents the best-fitting model. Residuals to the fit are shown in the lower panel.

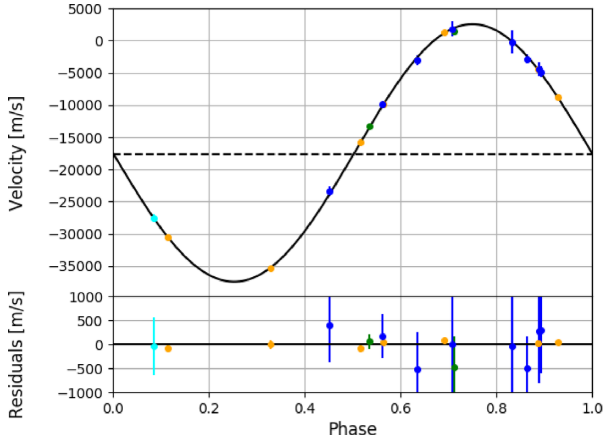

Figure 6. Phase folded RV measurements of EPIC 219654213 (Tull: blue; HIRES Blue: green; HIRES Red: cyan; FIES: yellow) and best-fitting model (black line). Residuals to the fit are shown in the lower panel.

SpecMatch-emp, we select the Dartmouth stellar models consistent with the stellar density according to our modelling results.

4 DISCUSSION

The binary system EPIC 219654213 consists of an F7V main sequence star orbited by an M5V star on nearly circular orbit with an orbital period of 5.441995 ± 0.000007 d. We can confirm a small but significant eccentricity of 0.0073 ± 0.0003. The radial velocity semi-amplitude of $K = 20.066 \pm 0.009\,\mathrm{km\,s^{-1}}$ together with the mass of the primary star ($1.008^{+0.081}_{-0.097}\,\mathrm{M_\odot}$) leads to a mass of the M dwarf companion of $0.187^{+0.012}_{-0.013}\,\mathrm{M_\odot}$. The radius of the M dwarf is $0.200^{+0.007}_{-0.008}\,\mathrm{R_\odot}$. The uncertainties in stellar parameters are model dependent as the bulk parameters of the primary star are based on Dartmouth isochrones.

4.1 Ruprecht 147 cluster membership

The open cluster Ruprecht 147 is an old nearby clusters (Curtis et al. 2013). Open clusters are a laboratory for stellar astrophysics. For members of open clusters we can constrain their age which would allow to give much better constrains for stellar evolution theories. This is why it is important to know whether EPIC 219654213 belongs to Ruprecht 147. The cluster membership for Ruprecht 147 has been analysed in the past as part of global catalogues of open clusters (e.g. Kharchenko et al. 2005; Dias et al. 2006, 2014) and in detail by Curtis et al. (2013). There is a discrepancy between results by Dias et al. (2014), who gives EPIC 219654213 a cluster membership probability of 83 per cent, and Curtis et al. (2013), who does not list EPIC 219654213 as a cluster member.

Using the GAIA DR2 catalogue (Gaia Collaboration 2018), we confirm the result of Curtis et al. (2013). Based on the GAIA DR2 five-parameter astrometry we identify 102 Cluster members which allow us to determine the distance of the Ruprecht 147 cluster to 310 ± 20 pc. The mean proper motion of the cluster is $pm_{ra} = -0.84 \pm 0.84\,\mathrm{mas\,yr^{-1}}$, $pm_{\mathrm{dec}} = -26.7 \pm 0.9\,\mathrm{mas\,yr^{-1}}$. The GAIA-DR2 astrometric solution for EPIC 219654213 however gives a distance of 1260 ± 50 pc and a proper motion of $pm_{ra} = 1.21 \pm 0.05\,\mathrm{mas\,yr^{-1}}$, and $pm_{\mathrm{dec}} = -8.62 \pm 0.04\,\mathrm{mas\,yr^{-1}}$ which is in agreement with EPIC 219654213 being a field star.

4.2 Relativistic beaming effect

As we can clearly see ellipsoidal variation, reflection, and the beaming effect in our light curve we also modelled the light-curve data without taking the spectroscopic RV data into account to compare the radial velocity determined spectroscopically to the radial velocity determined from the beaming effect. In this case we fixed the eccentricity to the value determined by our combined modelling as the depth of the secondary eclipse is close to the noise level and does not allow us to restrict the eccentricity.[6] The beaming factor is estimated using relations to the effective temperature and metallicity of the star (cf. Csizmadia submitted).

Fitting the light curve independent of the RV data, the best-fitting radial velocity semi-amplitude is $K_{\mathrm{LC}} = 13.7 \pm 0.7\,\mathrm{km\,s^{-1}}$ in comparison to the spectroscopic radial velocity $K = 20.066 \pm 0.009\,\mathrm{km\,s^{-1}}$ when fitting spectroscopic and photometric data together. The results are not in agreement with each other. The difference in the amplitude corresponding to the beaming effect of the respective radial velocity amplitude is $\Delta A_{\mathrm{Beam}} \approx 75$ ppm.

In our combined model the radial velocity semi-amplitude is dominated by the spectroscopic data, allowing us to use the combined model to determine the radial velocity semi-amplitude without being impaired by this discrepancy.

A possible explanation for the difference in radial velocity measured by the beaming effect and spectroscopic data might be the additional variability in the light curve which is not included in our model. Our light-curve model includes ellipsoidal variation, reflection, and the relativistic beaming effect. Additional brightness variations on the surface of the primary star might introduce further rotational variability, which in case of synchronized rotation would have the same period as the other effects. The rotational velocity of the primary star, estimated from $v \sin i_1$ and stellar radius, is in agreement with the system being tidally locked. As our model does not include rotational variability, the presence of such signal would

[6] We also modelled the light curve with the eccentricity fixed to $e = 0$ as a test case. As the eccentricity of the system is very small it had no major impact on the final results. To allow better comparison with our combined modelling we thus fixed the eccentricity to the value determined from the radial velocity follow up observations.

Table 3. Parameters from light curve and RV data analysis. Mass and radius of both components determined by combining modelling results with Dartmouth stellar models.

Parameter	Modelling result	Unit
Orbital period $P_{\rm orb}$	5.441995 ± 0.000007	d
Transit epoch T_0	2471.1452 ± 0.0002	$\rm BJD_{TDB} - 2450000$
Transit duration	4.58 ± 0.02	h
Scaled semimajor axis a/R_*	9.07 ± 0.03	–
Semimajor axis a	0.065 ± 0.003	au
Scaled secondary radius R_2/R_1	0.1320 ± 0.0003	–
Orbital inclination angle i	89.70 ± 0.23	deg
Conjunction parameter b_c	0.05 ± 0.04	–
Limb-darkening coefficient u_+	0.6 (fixed)	–
Limb-darkening coefficient u_-	0.2 (fixed)	–
Brightness ratio	0.026 ± 0.005	–
Albedo of primary star	0.71 ± 0.17	–
Albedo of secondary star	0.30 ± 0.20	–
Ellipsoidal variability term a_1	0.00059 ± 0.00001	–
Ellipsoidal variability term a_2	-0.00006 ± 0.00004	–
Ellipsoidal variability term a_3	0.00005 ± 0.00004	–
Ellipsoidal variability term a_4	-0.00001 ± 0.00004	–
Ellipsoidal variability term a_5	0.00007 ± 0.00004	–
Radial velocity semi-amplitude K	20.066 ± 0.009	$\rm km\,s^{-1}$
Systemic radial velocity γ	-17.57 ± 0.07	$\rm km\,s^{-1}$
RV velocity offset FIES / Tull	30.48 ± 0.07	$\rm km\,s^{-1}$
RV velocity offset HIRES Blue / Tull	0.18 ± 0.07	$\rm km\,s^{-1}$
RV velocity offset HIRES Red / Tull	-0.95 ± 0.15	$\rm km\,s^{-1}$
Eccentricity e	0.0073 ± 0.0003	–
Primary mass M_1	$1.008^{+0.081}_{-0.097}$	$\rm M_\odot$
Primary radius R_1	$1.518^{+0.038}_{-0.049}$	$\rm R_\odot$
Secondary mass M_2	$0.187^{+0.012}_{-0.013}$	$\rm M_\odot$
Secondary radius R_2	$0.200^{+0.007}_{-0.008}$	$\rm R_\odot$

be compensated by adapting the ellipsoidal variation, the beaming effect, and the reflection.

As we expect rotational variability to be changing over timescales of a few rotations, we tested this assumption by splitting the light curve into two segments and modelling these segments independently. The results show a change in the amplitude of the beaming effect of 35 ppm, which account for 50 per cent of the observed discrepancy between expected and observed beaming effect. This shows that the systematic error in modelling the beaming effect is much larger than is reflected in the value of $K_{\rm LC} = 13.7 \pm 0.7\,\rm km\,s^{-1}$, but still might not explain the whole offset. For rotational variability to be causing this offset, there would need to be a contribution that is stable over the whole observation, which might be if it is introduced by interactions between the two stars.

We tested whether the uncertainty in third light diluting our signal could also explain the observed discrepancy, but the effect would be an order of magnitude to small.

4.3 Low mass stars mass–radius relation

Using spectroscopic radial velocity measurements in combination with a high-precision light curve we were able to determine the mass and radius of the companion with only a few percent uncertainty. The mass radius relation of the M-dwarf is in the range predicted by stellar models for stars of this age. EPIC 219654213B with a mass of $0.187^{+0.012}_{-0.013}$ $\rm M_\odot$ is one of only few characterized very low mass stars in eclipsing binaries.

5 CONCLUSIONS

We discovered an eclipsing binary star EPIC 219654213, consisting of an M5V orbiting an F7V star. EPIC 219654213 is not a member of the cluster Ruprecht 147. High-precision photometry by the K2 mission and radial velocity data allowed to characterize the system and both components. The M5V star has a mass of $M_2 = 0.187^{+0.012}_{-0.013}\,\rm M_\odot$ and a radius of $R_2 = 0.200^{+0.007}_{-0.008}\,\rm R_\odot$. The primary star has a mass of $M_1 = 1.008^{+0.081}_{-0.097}\,\rm M_\odot$ and a radius of $R_2 = 1.518^{+0.038}_{-0.049}\,\rm R_\odot$. The high-precision photometry allowed us to observe also the photometric beaming effect. Its amplitude is not in agreement with the radial velocity measured spectroscopically. Using the beaming effect to determine the mass of the secondary objects gives $M_{\rm 2LC} = 0.13 \pm 0.04\,\rm M_\odot$, which underestimates the mass by ≈35 per cent. However, detailed analysis of the light curve showed that the amplitude of the out-of-transit variation changes with time which might hint towards the presence of additional variability in our light curve, preventing us from using beaming to estimate the mass of the companion. Especially for short period binaries, where the rotational period is synchronized with the orbital period this might be a common effect. This shows how careful one has to treat the beaming effect when using it to determine the mass of the secondary object. However, for surveys spanning over several orbital periods, a detailed analysis might help to estimate the mass, taking additional stellar variability into account.

The upcoming *TESS* and future *PLATO* mission are expected to deliver large numbers of planetary candidates, thus resources for spectroscopic follow up will be limited. For cases such as EPIC 219654213 mass estimate of the secondary object will be needed

to distinguish between the companion being an highly inflated hot Jupiter, late M-dwarf, and brown dwarf. It therefore has been proposed to classify such systems without spectroscopic radial velocity follow up by using the beaming effect. Our analysis shows that this needs to be done with care. Additional variability needs to be taken into account and might prevent us from proper modelling of the beaming effect.

ACKNOWLEDGEMENTS

This paper includes data collected by the K2 mission. Funding for the K2 mission is provided by the NASA Science Mission directorate.

This paper is based on observations made with the Nordic Optical Telescope, operated by the Nordic Optical Telescope Scientific Association at the Observatorio del Roque de los Muchachos, La Palma, Spain, of the Instituto de Astrofisica de Canarias.

This paper includes data taken at The McDonald Observatory of The University of Texas at Austin.

Some of the data presented herein were obtained at the W. M. Keck Observatory, which is operated as a scientific partnership among the California Institute of Technology, the University of California, and the National Aeronautics and Space Administration. The Observatory was made possible by the generous financial support of the W. M. Keck Foundation. The authors wish to recognize and acknowledge the very significant cultural role and reverence that the summit of Maunakea has always had within the indigenous Hawaiian community. We are most fortunate to have the opportunity to conduct observations from this mountain.

This work has made use of data from the European Space Agency (ESA) mission *Gaia* (https://www.cosmos.esa.int/gaia), processed by the *Gaia* Data Processing and Analysis Consortium (DPAC, https://www.cosmos.esa.int/web/gaia/dpac/consortium). Funding for the DPAC has been provided by national institutions, in particular the institutions participating in the *Gaia* Multilateral Agreement.

HJD acknowledges support by grant ESP2015-65712-C5-4-R of the Spanish Secretary of State for R&D&i (MINECO).

ME and WDC were supported by NASA grant NNX16AE70G to The University of Texas at Austin.

REFERENCES

Barragán O. et al., 2016, AJ, 152, 193
Bloemen S. et al., 2011, MNRAS, 410, 1787
Borucki W. J. et al., 2010, Science, 327, 977
Bressan A., Marigo P., Girardi L., Salasnich B., Dal Cero C., Rubele S., Nanni A., 2012, MNRAS, 427, 127
Cabrera J., Csizmadia S., Erikson A., Rauer H., Kirste S., 2012, A&A, 548, A44
Chaturvedi P., Sharma R., Chakraborty A., Anandarao B. G., Prasad N. J. S. S. V., 2018, AJ, 156, 27
Csizmadia S. et al., 2015, A&A, 584, A13
Curtis J. L., Wolfgang A., Wright J. T., Brewer J. M., Johnson J. A., 2013, AJ, 145, 134
Dias W. S., Assafin M., Flório V., Alessi B. S., Líbero V., 2006, A&A, 446, 949
Dias W. S., Monteiro H., Caetano T. C., Lépine J. R. D., Assafin M., Oliveira A. F., 2014, A&A, 564, A79
Dotter A., Chaboyer B., Jevremović D., Kostov V., Baron E., Ferguson J. W., 2008, ApJS, 178, 89
Eigmüller P. et al., 2016, AJ, 151, 84
Eigmüller P. et al., 2017, AJ, 153, 130
Endl M., Cochran W. D., 2016, PASP, 128, 94502
Faigler S., Kull I., Mazeh T., Kiefer F., Latham D. W., Bloemen S., 2015, ApJ, 815, 26
Gaia Collaboration, Brown A. G. A. , Vallenari A., Prusti T., de Bruijne J. H. J., Babusiaux C., Bailer-Jones C. A. L., 2018, preprint (arXiv: 1804.09365)
Gandolfi D. et al., 2015, A&A, 576, A11
Gillen E., Hillenbrand L. A., David T. J., Aigrain S., Rebull L., Stauffer J., Cody A. M., Queloz D., 2017, ApJ, 849, 11
Grziwa S. et al., 2016a, AJ, 152, 132
Herrero E., Lanza A. F., Ribas I., Jordi C., Collier Cameron A., Morales J. C., 2014, A&A, 563, A104
Howell S. B. et al., 2014, PASP, 126, 398
Jofré E., Petrucci R., Saffe C., Saker L., de la Villarmois E. A., Chavero C., Gómez M., Mauas P. J. D., 2015, A&A, 574, A50
Johnson M. C. et al., 2016, AJ, 151, 171
Kharchenko N. V., Piskunov A. E., Röser S., Schilbach E., Scholz R. D., 2005, A&A, 438, 1163
Loeb A., Gaudi B. S., 2003, ApJ, 588, L117
Mandel K., Agol E., 2002, ApJ, 580, L171
Mann A. W., Feiden G. A., Gaidos E., Boyajian T., von Braun K., 2015, ApJ, 804, 64
Mazeh T., Faigler S., 2010, A&A, 521, L59
Smith A. M. S. et al., 2017, MNRAS, 464, 2708
Southworth J., 2015, in Rucinski S. M., Torres G., Zejda M., eds, ASP Conf. Ser. Vol. 496, DEBCat: A Catalog of Detached Eclipsing Binary Stars. Astron. Soc. Pac., San Francisco, p. 164
Tal-Or L., Faigler S., Mazeh T., 2015, A&A, 580, A21
Telting J. H. et al., 2014, Astron. Nachr., 335, 41
Tody D., 1993, in Hanisch R. J., Brissenden R. J. V., Barnes J., eds, ASP Conf. Ser. Vol. 52, Astronomical Data Analysis Software and Systems II. Astron. Soc. Pac., San Francisco, p. 173.
Tull R. G., MacQueen P. J., Sneden C., Lambert D. L., 1995, PASP, 107, 251
Udry S., Mayor M., Queloz D., 1999, in Hearnshaw J. B., Scarfe C. D., eds, ASP Conf. Ser. Vol. 185: Precise Stellar Radial Velocities. Astron. Soc. Pac., San Francisco, p. 367.
van Kerkwijk M. H., Rappaport S. A., Breton R. P., Justham S., Podsiadlowski P., Han Z., 2010, ApJ, 715, 51
Vanderburg A., Johnson J. A., 2014, PASP, 126, 948
Vogt S. S. et al., 1994, in Crawford D. L., Craine E. R., eds, Proc. SPIE Conf. Ser. Vol. 2198, Instrumentation in Astronomy VIII. SPIE, Bellingham, p. 362
Yee S. W., Petigura E. A., von Braun K., 2017, ApJ, 836, 77
Zucker S., Mazeh T., Alexander T., 2007, ApJ, 670, 1326

This paper has been typeset from a TEX/LATEX file prepared by the author.